bind to the specific Ca^{2+}-binding site(s) of CaM under our experiiental conditions, although ionic valence numbers, effective ionic radii, binding constants, and coordination structures of these cations are different from each other.[32,35] The very specific role of Ca^{2+} in intracellular Ca^{2+}-related functions may be due to its ability to cause hydrophobic character of Ca^{2+}-dependent proteins. Very variable bond lengths and coordination numbers of Ca^{2+} compared with other metal cations may be related to the specific character of Ca^{2+}.[30,32,35] It should be emphasized here that the quadrupole metal NMR method is quite useful for obtaining individual information on each metal binding site in macromolecules.

Acknowledgment. This work was supported in part by Grants-in-Aid for Scientific Research from the Ministry of Education, Science and Culture, Japan, and by a grant from Nissan Science Foundation to M.H.

Registry No. ^{43}Ca, 14333-06-3; ^{25}Mg, 14304-84-8; ^{67}Zn, 14378-34-8; ^{39}K, 14092-91-2; Ca, 7440-70-2; Mg, 7439-95-4; Zn, 7440-66-6; K, 7440-09-7; TFP, 117-89-5.

Supplementary Material Available: A figure showing temperature dependences of ^{43}Ca, ^{25}Mg, and ^{67}Zn NMR line widths for Ca^{2+}–, Mg^{2+}–, and Zn^{2+}–CaM solutions (2 pages). Ordering information is given any current masthead page.

Contribution from the Department of Chemistry,
University of Massachusetts, Amherst, Massachusetts 01003

Synthesis and Molecular Structure of Five-Coordinated Spirocyclic Anionic Silicates Containing *tert*-Butyl Groups. Hydrogen-Bonding Effects[1,2]

ROBERT R. HOLMES,* ROBERTA O. DAY, V. CHANDRASEKHAR, and JOAN M. HOLMES

Received August 28, 1984

The new five-coordinated anionic silicates $[((t\text{-Bu})_2C_6H_2O_2)_2SiPh][Et_3NH]$ (**1**), $[(C_6H_4O_2)_2SiPh][Et_3NH]$ (**2**), and $[(C_{10}H_6O_2)_2Si\text{-}t\text{-}Bu][Et_4N]$ (**3**) were synthesized and their X-ray structures obtained. ^{1}H, ^{29}Si, and ^{13}C NMR spectral data also are reported. The structures are displaced 29.0% for **1**, 59.4% for **2**, and 80.3% for **3** from the trigonal bipyramid toward the rectangular pyramid (based on unit bond distances). It is concluded that hydrogen bonding between the ammonium cation and oxygen atoms of the spirocyclic framework, e.g. in **2**, causes displacement of the structural form toward the rectangular pyramid compared to related structures lacking this hydrogen-bonding possibility. It is felt that the use of *tert*-butyl ring substituents in **1** shields the silicon center from the hydrogen-bonding effect of the cation and, hence, accounts for the near-trigonal-bipyramidal geometry observed. Details of this form of the distortion coordinate are presented and shown to be closely related to nonrigid phosphoranes and arsoranes. **1** crystallizes in the orthorhombic space group $P2_12_12_1$ with $a = 11.849$ (1) Å, $b = 17.040$ (2) Å, $c = 19.857$ (3) Å, and $Z = 4$. **2** crystallizes in the monoclinic space group $P2_1/n$ with $a = 10.492$ (2) Å, $b = 21.104$ (5) Å, $c = 10.598$ (1) Å, $\beta = 98.92$ (1)°, and $Z = 4$. **3** crystallizes in the monoclinic space group $P2_1/n$ with $a = 9.678$ (2) Å, $b = 25.368$ (7) Å, $c = 12.909$ (3) Å, $\beta = 108.18$ (2)°, and $Z = 4$. The final conventional unweighted residuals are 0.065 (**1**), 0.042 (**2**), and 0.081 (**3**).

Introduction

We have shown that the molecular structures of pentacoordinated anionic silicon complexes[3,4] follow the same type of distortion coordinate as observed for isoelectronic phosphoranes,[5,7] i.e., the Berry pseudorotational coordinate that connects the ideal trigonal bipyramid (TBP) with a square or rectangular pyramid (RP). The latter coordinate has been supported as the principal one accounting for NMR ligand-exchange phenomena in a wide variety of pentacoordinated phosphorus compounds.[8,9] This same coordinate is followed by the structures of arsoranes[1,10] and five-coordinated germanium compounds so far examined.[11] In all of these cases, a trans basal angle, θ, near 150° is indicated for the geometry of the "ideal" square pyramid. This contrasts with that found for five-coordinated transition-metal derivatives that show θ angles varying from 140 to 175°.[12,13]

The general features that stabilize the normally higher energy square pyramid for phosphoranes[6,7,14] are found to apply equally well to the less well-studied five-coordinated silicon[3] compounds. Most of the observed structural distortions are consistent with expectations from substituent effects.[3,4,6,7,15] However, unlike the molecular phosphoranes, the isoelectronic five-coordinated silicates have additional complicating features owing to the saltlike character of the complexes and the presence of hydrogen bonding between hydrogen-containing cations and oxygen atoms of the silicon anion.

In this paper, an attempt is made to evaluate the role of these two lattice effects in influencing the geometrical distortion of pentacoordinated silicon compounds. The compounds chosen for study are $[((t\text{-Bu})_2C_6H_2O_2)_2SiPh][Et_3NH]$ (**1**), $[(C_6H_4O_2)_2SiPh][Et_3NH]$ (**2**), and $[(C_{10}H_6O_2)_2Si\text{-}t\text{-}Bu][Et_4N]$ (**3**).

The first structure of an anionic silicate compound that was established was an X-ray study of **4** performed in 1968.[16] The geometry is displaced approximately one-third the way from the TBP.[3] The numbers in parentheses below the formula representations are the percent displacement along the Berry coordinate from the TBP toward the RP calculated by a dihedral angle

---

(1) Pentacoordinated Molecules. 61. Part 60: Holmes, R. R.; Day, R. O.; Sau, A. C. *Organometallics* **1985**, *4*, 714.

(2) Presented at the Seventh International Symposium on Organosilicon Chemistry, Kyoto, Japan, Sept 1984; Chemical Society of Japan, Abstr. 2C1110.

(3) Holmes, R. R.; Day, R. O.; Harland, J. J.; Sau, A. C.; Holmes, J. M. *Organometallics* **1984**, *3*, 341.

(4) Holmes, R. R.; Day, R. O.; Harland, J. J.; Holmes, J. M. *Organometallics* **1984**, *3*, 347.

(5) Holmes, R. R. "Pentacoordinated Phosphorus", *ACS Monogr.* **1980**, *175*.

(6) Holmes, R. R. *Acc. Chem. Res.* **1979**, *12*, 257 and references cited therein.

(7) Holmes, R. R.; Deiters, J. A. *J. Am. Chem. Soc.* **1977**, *99*, 3318.

(8) Cited in: Holmes, R. R. *ACS Monogr.* **1980**, *175*, Chapter 3.

(9) Holmes, R. R. *J. Am. Chem. Soc.* **1974**, *96*, 4143.

(10) Poutasse, C. A.; Day, R. O.; Holmes, J. M.; Holmes, R. R. *Organometallics* **1985**, *4*, 708.

(11) Holmes, R. R.; Day, R. O.; Sau, A. C.; Poutasse, C. A.; Holmes, J. M. *Inorg. Chem.* **1985**, *24*, 193.

(12) Holmes, R. R. *J. Am. Chem. Soc.* **1984**, *106*, 3745.

(13) Holmes, R. R. *Prog. Inorg. Chem.* **1984**, *32*, Chapter 2.

(14) Holmes, R. R. *J. Am. Chem. Soc.* **1975**, *97*, 5379.

(15) Cited in: Holmes, R. R. *ACS Monogr.* **1980**, *175*, 43–49.

(16) Boer, F. P.; Flynn, J. J.; Turley, J. W. *J. Am. Chem. Soc.* **1968**, *90*, 6973.

0020-1669/85/1324-2009$01.50/0 © 1985 American Chemical Society

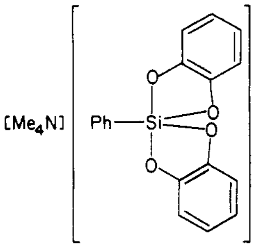

4 (29.5%)

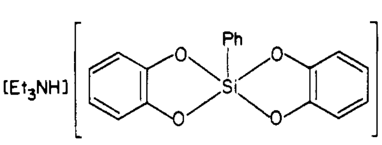

2

method based on unit bond distances.[6,7,17] For comparison, the related complex, **2**, containing hydrogen-bonding possibilities was synthesized and its X-ray structure determined. When *tert*-butyl groups are introduced on the cyclic portion of the silicate, the more sterically shielded formulation **1** is obtained that should experience a decreased lattice effect caused by the cation in influencing the geometry at the silicon center. Last, the structure of the *tert*-butyl derivative, **3**, lacking hydrogen-bonding consequences, was determined for comparison with the analogous silicate, **5**,[4] exhibiting hydrogen bonding.

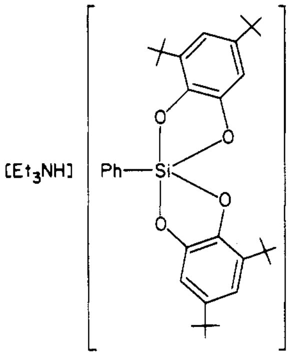

1

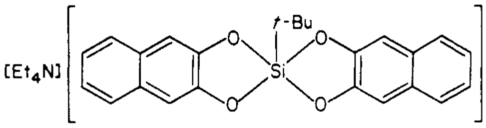

3

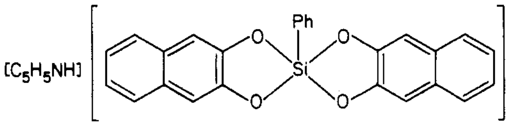

5 (97.6%)

Experimental Section

Proton NMR spectra were recorded with a Varian Model XL-300 NMR spectrometer operating at 300 MHz using pulse FT methods. The samples were dissolved in CD_3CN. ^{29}Si NMR spectra were obtained on the XL-300 spectrometer at 59.6 MHz operating in the Fourier transform mode. Samples were prepared in acetonitrile (0.5–1.0 M) containing $Cr(acac)_3$ (0.04 M) to reduce relaxation times. ^{13}C NMR were recorded on a Varian Model XL-200 NMR spectrometer operating in the FT mode at 50.31 MHz. The samples were dissolved in acetonitrile. Deuteriochloroform was used for locking, with Me_4Si as the internal standard. The chemical shifts are reported in ppm; shifts downfield to Me_4Si are positive.

The ^{13}C assignments are tentative. They are based on reported trends and general additivity rules for organosilicon compounds.[18,19] The numbering system for the aromatic substituents used for the ^{13}C assignments is shown:

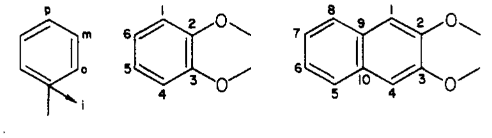

Materials. Catechol, 2,3-naphthalenediol, and 3,5-di-*tert*-butylcatechol (Aldrich) were used as received. Tetraethylammonium halides (Eastman Kodak) were dried over P_2O_5 under vacuum before use. Solvents were purified by conventional methods. Phenyltrimethoxysilane and *tert*-butyl-trichlorosilane (Petrarch) were used as received.

Preparations. (a) Triethylammonium Bis(3,5-di-*tert*-butyl-1,2-benzenediolato)phenylsilicate(IV), [((*t*-Bu)$_2$C$_6$H$_2$O$_2$)$_2$SiPh][Et$_3$NH] (1). A solution of 3,5-di-*tert*-butylcatechol (2.39 g, 10.8 mmol) in methanol (20 mL) and acetonitrile (20 mL) was reacted with phenyltrimethoxysilane (1.07 g, 5.4 mmol) and triethylamine (0.54 g, 5.4 mmol) at 70 °C for 20 min. Removal of solvent yielded a solid. It was recrystallized from a mixture of acetonitrile and ether (1:3) at 0 °C: yield 3.2 g (91.5%); mp 198 °C dec. ^{1}H NMR (δ): 1.25 (t, $NCCH_3$, 9 H), 1.35 (s, CCH_3, 36 H), 3.12 (q, NCH_2CH_3, 6 H); (aromatic signals) 6.65 (m, 4 H), 7.15 (m, meta and para protons of the phenyl ring), 7.60 (m, ortho protons of the phenyl ring). ^{29}Si NMR (δ): −87.8. ^{13}C NMR for the anion (δ): C_i, 138.37; C_o, 134.16; C_m, 126.06; C_p, 127.16; C_1/C_5, 131.10; C_2/C_3, 148.24, 145.20; C_4/C_6, 115.77, 115.60. ^{13}C NMR for the cation (δ): NC*C*, 8.0; N*C*C, 45.93. Anal. Calcd for $C_{40}H_{61}O_4NSi$: C, 74.14; H, 9.45; N, 2.16. Found: C, 73.94; H, 9.40; N, 2.10.

(b) Triethylammonium Bis(*o*-phenylenedioxy)phenylsilicate(IV), [(C$_6$H$_4$O$_2$)$_2$SiPh][Et$_3$NH] (2). This compound was prepared by Frye[20] earlier. Phenyltrimethoxysilane (0.99 g, 5 mmol) was reacted with catechol (1.1 g, 10 mmol) and triethylamine (0.51 g, 5 mmol) in acetonitrile (50 mL) and methanol (30 mL) at 70 °C for 1 h. Removal of solvent yielded a whitish crystalline solid. It was recrystallized from acetonitrile and ether (1:3): yield 1.70 g (80.2%); mp 220 °C dec. ^{1}H NMR (δ): 1.03 (t, $NCCH_3$, 9 H), 2.97 (q, NCH_2CH_3, 6 H); (aromatic signals) 6.70 (m, 8 H), 7.13 (m, meta and para protons of the phenyl ring), 7.54 (m, ortho protons of the phenyl ring). ^{29}Si NMR (δ): −87.0. ^{13}C NMR for the anion (δ): C_i, 139.61; C_o, 134.50; C_m, 127.21; C_p, 128.61; C_1/C_4, 110.70; C_2/C_3, 149.53; C_5/C_6, 118.8. Anal. Calcd for $C_{24}H_{29}O_4NSi$: C, 68.05; H, 6.90; N, 3.31. Found: C, 67.94; H, 7.01; N, 3.27.

(c) Tetraethylammonium Bis(2,3-naphthalenediolato)-*tert*-butylsilicate(IV), [(C$_{10}$H$_6$O$_2$)$_2$Si-*t*-Bu][Et$_4$N] (3). *tert*-Butyltrichlorosilane (1.10 g, 5.7 mmol) was reacted with 2,3-naphthalenediol (1.84 g, 11.4 mmol) and triethylamine (2.32 g, 22.9 mmol) in benzene (200 mL) under reflux for 12 h. A white precipitate that was formed in the reaction was filtered under suction and treated with water (3 × 50 mL) to remove triethylamine hydrochloride. Tetraethylammonium chloride (0.95 g, 5.7 mmol) was added to a suspension of the insoluble portion in acetone (50 mL), and the reaction mixture was heated under reflux for $^1/_2$ h. Removal of solvent yielded a semisolid that was treated with water (2 × 50 mL) to remove the metathetically exchanged triethylamine hydrochloride. The remaining portion was redissolved in acetone and dried (Na_2SO_4) and solvent removed to give **3**, yield, 2.5 g (81.9%). It was recrystallized from a mixture of acetonitrile and ether (1:3) at 0 °C; melting range 150–153 °C. ^{1}H NMR (δ): 0.82 (s, CCH_3, 9 H), 1.15 (t, NCH_2CH_3, 12 H), 3.07 (q, NCH_2CH_3, 8 H); (aromatic region) 7.20 (m, 4 H), 7.54 (m, 4 H), 7.60 (m, 4 H). ^{13}C NMR for the anion (δ): *C*CH$_3$, 27.86; C*C*H$_3$, 28.03; C_1/C_4, 125.13; C_2/C_3, 151.40; C_5/C_8, 122.68; C_6/C_7, 121.09; C_9/C_{10}, 128.89. ^{13}C NMR for the cation (δ): NC*C*, 6.32; N*C*C, 51.45. Anal. Calcd for $C_{32}H_{41}NO_4Si$: C, 72.28; H, 7.77; N, 2.63. Found: C, 71.87; H, 7.65; N, 2.70.

X-ray Studies. All X-ray crystallographic studies were done on an Enraf-Nonius CAD4 diffractometer with graphite-monochromated molybdenum radiation at an ambient temperature of 23 ± 2 °C. The weighted average, $\lambda(K\bar{\alpha}) = 0.71073$ Å, is the wavelength used for the calculation of the lattice constants. Details of the experimental and computational procedures have been described previously.[21]

Crystals were mounted in sealed thin-walled glass capillaries as a precaution against moisture sensitivity. Diffraction data were collected in the θ–2θ scan mode for $2° \leq 2\theta_{Mo K\bar{\alpha}} \leq 43°$. No corrections were made for absorption. The structures were solved by a combination of direct methods (MULTAN) and standard difference Fourier techniques and were

---

(17) Cited in: Holmes, R. R. *ACS Monogr.* **1980**, *175*, pp. 34–42.

(18) (a) Harris, R. K.; Jones, J.; Ng, S. *J. Magn. Reson.* **1978**, *30*, 521. (b) Rakita, P. E.; Worsham, L. S.; Srebro, J. P. *Org. Magn. Reson.* **1976**, *8*, 310; (c) Rakita, P. E.; Worsham, L. S. *J. Organomet. Chem.* **1977**, *139*, 135; (d) Rakita, P. E.; Worsham, L. S. *J. Organomet. Chem.* **1977**, *137*, 145.

(19) Stothers, J. B. "Carbon-13 NMR Spectroscopy"; Academic Press, New York, 1972.

(20) Frye, C. L. *J. Am. Chem. Soc.* **1964**, *86*, 3170.

(21) Sau, A. C.; Day, R. O.; Holmes, R. R. *Inorg. Chem.* **1981**, *20*, 3076. Computations were done on a CDC Cyber-175 computer using LINEX, a modification of the Busing and Levy full-matrix least-squares program, ORFLS, Johnson's thermal ellipsoid plot program, ORTEP, the Oak Ridge Fortran function and error program, ORFFE, Zalkin's Fourier program, FORDAP, and several locally written programs.

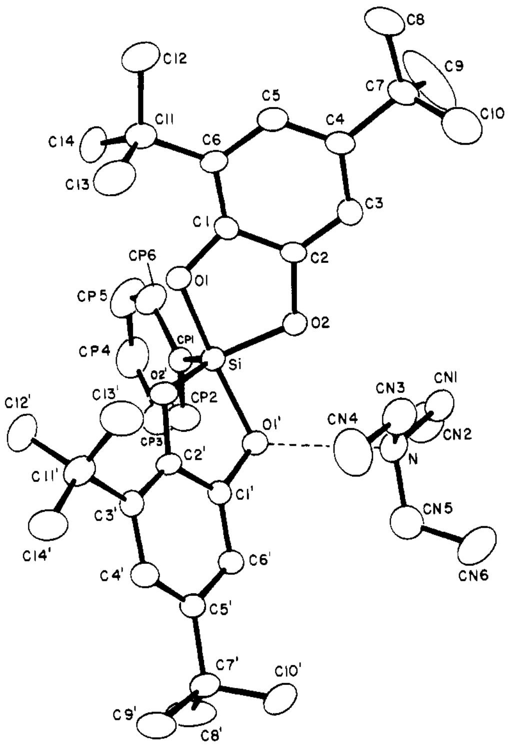

Figure 1. ORTEP plot of $[((t\text{-Bu})_2C_6H_2O_2)_2SiPh][Et_3NH]$ (1) with thermal ellipsoids at the 30% probability level. Atoms of the cation shown are related to those in the coordinate list by $\frac{1}{2} + x$, $1\frac{1}{2} - y$, $\frac{1}{2} - z$. Hydrogen atoms are omitted for purposes of clarity. The presence of the H-bonding interaction is indicated by the dashed line.

refined by using full-matrix least squares.[22]

X-ray Crystallographic Studies for $[((t\text{-Bu})_2C_6H_2O_2)_2SiPh][Et_3NH]$ (1). Large colorless striated needles obtained by crystallization from CH_2Cl_2/Skelly F (1:1) diffract poorly. The crystal used for data collection was cut to approximate dimensions of 0.26 × 0.31 × 0.43 mm.

Crystal Data for $C_{40}H_{61}O_4NSi$ (1): uniquely determined orthorhombic space group $P2_12_12_1$ [D_2^4-No. 19],[23] $a = 11.849$ (1) Å, $b = 17.040$ (2) Å, $c = 19.857$ (3) Å, $Z = 4$, $\mu_{\text{Mo K}\alpha} = 0.0998$ mm^{-1}; total of 2613 independent reflections ($+h,+k,+l$) measured.

The 46 independent non-hydrogen atoms were refined anisotropically. The 15 independent aromatic and methylene hydrogen atoms were included in the refinement as fixed isotropic scatterers with calculated coordinates that were updated as refinement converged so that the final C–H bond lengths were 0.98 Å. The remaining hydrogen atoms were omitted from the refinement. The final agreement factors[24] were $R = 0.065$ and $R_w = 0.088$ for the 2199 reflections having $I \geq 2\sigma_I$. A final difference Fourier synthesis showed a maximum density of 0.273 e/Å^3.

X-ray Crystallographic Studies for $[(C_6H_4O_2)_2SiPh][Et_3NH]$ (2). Poorly formed colorless rods were obtained by crystallization from CH_3CN/Et_2O (1:3). A piece cut from one of these (0.33 × 0.35 × 0.48 mm) was used for data collection. A different crystalline form[25] was obtained by crystallization from C_6H_6/Et_2O.

Crystal Data for $C_{24}H_{29}O_4NSi$ (2): uniquely determined monoclinic space group $P2_1/n$ (alternate setting of $P2_1/c$ [C_{2h}^5-No. 14][26]), $a = 10.492$ (2) Å, $b = 21.104$ (5) Å, $c = 10.598$ (1) Å, $\beta = 98.92$ (1)°, $Z = 4$, $\mu_{\text{Mo K}\alpha} = 0.134$ mm^{-1}; total of 2659 independent reflections ($+h,+k,\pm l$) measured.

The 30 independent non-hydrogen atoms were refined anisotropically. The 19 independent aromatic and methylene hydrogen atoms were treated in the same manner as for 1. Coordinates for the nine independent methyl hydrogen atoms and the N–H hydrogen atom, HN, were obtained from a difference Fourier synthesis. Methyl hydrogen atoms were included in the refinement as fixed isotropic scatterers, while the parameters for HN were refined. The final agreement factors[24] were $R = 0.042$ and $R_w = 0.045$ for the 2008 reflections having $I \geq 2\sigma_I$. The maximum density on a final difference Fourier synthesis was 0.191 e/Å^3.

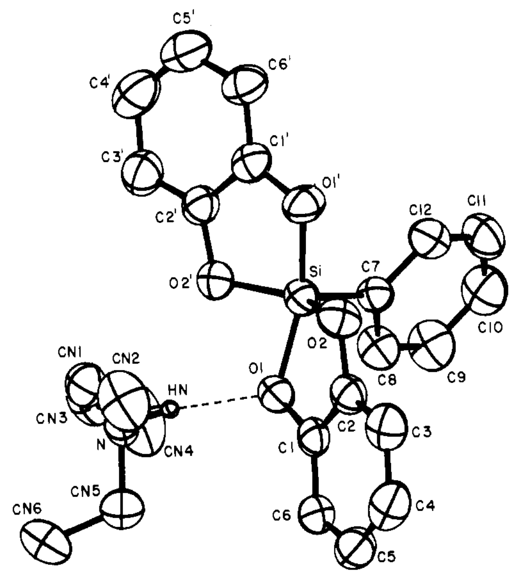

Figure 2. ORTEP plot of $[(C_6H_4O_2)_2SiPh][Et_3NH]$ (2) with thermal ellipsoids at the 50% probability level. Hydrogen atoms, except for HN, have been omitted for purposes of clarity. The hydrogen bond is shown as a dashed line. HN is represented as a sphere of arbitrary radius.

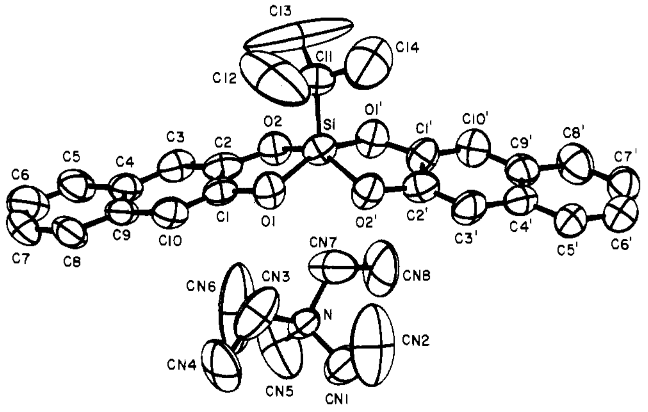

Figure 3. ORTEP plot of $[(C_{10}H_6O_2)_2Si\text{-}t\text{-Bu}][Et_4N]$ (3) with thermal ellipsoids at the 50% probability level. Hydrogen atoms are omitted for purposes of clarity.

X-ray Crystallographic Studies for $[(C_{10}H_6O_2)_2Si\text{-}t\text{-Bu}][Et_4N]$ (3). Clusters of colorless laths, obtained by crystallization from CH_3CN/Et_2O (1:3), diffract poorly. The crystal used for data collection was cut to approximate dimensions of 0.24 × 0.34 × 0.49 mm.

Crystal Data for $C_{32}H_{41}O_4NSi$ (3): uniquely determined monoclinic space group $P2_1/n$ (alternate setting of $P2_1/c$ [C_{2h}^5-No. 14][26]), $a = 9.678$ (2) Å, $b = 25.368$ (7) Å, $c = 12.909$ (3) Å, $\beta = 108.18$ (2)°, $Z = 4$, $\mu_{\text{Mo K}\alpha} = 0.118$ mm^{-1}; total of 3417 independent reflections ($+h,+k,\pm l$) measured.

The 38 independent non-hydrogen atoms were refined anisotropically. The 20 independent aromatic and methylene hydrogen atoms were treated in the same manner as for 1. Methyl hydrogen atoms were omitted from the refinement. The final agreement factors[24] were $R = 0.081$ and $R_w = 0.099$ for the 2072 reflections having $I \geq 2\sigma_I$. A final difference Fourier synthesis showed a maximum density of 0.541 e/Å^3.

Results

The atom-labeling scheme for 1 is given in the ORTEP plot of Figure 1. Atomic coordinates are given in Table I, while selected bond lengths and angles are given in Table II. The corresponding information for 2 is given in Figure 2 and in Tables III and IV and for 3 in Figure 3 and in Tables V and VI. For all three compounds, anisotropic thermal parameters, hydrogen atom parameters, additional bond lengths and angles, and deviations from

---

(22) The function minimized was $\sum w(|F_o| - |F_c|)^2$, where $w^{1/2} = 2F_oLp/\sigma_I$. Mean atomic scattering factors were taken from ref 23 (1974, Vol. IV, pp 72–98). Real and imaginary dispersion corrections for Si and O were taken from the same source (pp 149–150).

(23) "International Tables for X-ray Crystallography", Kynoch Press: Birmingham, England, 1969; Vol. I, p 105.

(24) $R = \sum||F_o| - |F_c||/\sum|F_o|$ and $R_w = \{\sum w(|F_o| - |F_c|)^2/\sum w|F_o|^2\}^{1/2}$. The R and R_w values for 1 are for the configuration having the lowest R_w.

(25) Space group $P2_1/c$, $a = 21.316$ (4) Å, $b = 13.320$ (2) Å, $c = 18.262$ (3) Å, $\beta = 107.79$ (1)°. This form degraded rapidly during data collection, and the study was abandoned.

(26) Cited in reference 23, p 99.

Table I. Atomic Coordinates in Crystalline $[((t\text{-Bu})_2C_6H_2O_2)_2SiPh][Et_3NH]$ (**1**)[a]

atom type[b]	10^4x	10^4y	10^4z
Si	9670 (2)	8424 (1)	3828.8 (9)
O1	10217 (4)	7864 (3)	3170 (2)
O2	9694 (4)	7599 (3)	4331 (2)
O1′	9390 (4)	8977 (3)	4595 (2)
O2′	10741 (4)	9068 (3)	3681 (2)
N	4883 (5)	6808 (4)	4196 (3)
C1	10332 (6)	7092 (4)	3318 (3)
C2	10040 (6)	6925 (4)	3981 (3)
C3	10070 (7)	6199 (4)	4242 (4)
C4	10467 (7)	5591 (4)	3835 (4)
C5	10814 (7)	5769 (4)	3180 (4)
C6	10767 (6)	6528 (4)	2906 (3)
C7	10475 (9)	4734 (5)	4105 (4)
C8	11099 (18)	4188 (6)	3640 (6)
C9	9245 (12)	4447 (7)	4169 (10)
C10	11010 (16)	4712 (7)	4804 (6)
C11	11191 (7)	6720 (5)	2193 (4)
C12	11633 (11)	5986 (6)	1826 (5)
C13	12195 (9)	7306 (7)	2271 (6)
C14	10220 (9)	7075 (5)	1769 (4)
C1′	9965 (5)	9678 (4)	4595 (3)
C2′	10773 (6)	9718 (4)	4091 (3)
C3′	11524 (5)	10331 (4)	4041 (3)
C4′	11373 (6)	10938 (4)	4507 (4)
C5′	10530 (6)	10935 (4)	5002 (3)
C6′	9814 (6)	10276 (4)	5040 (3)
C7′	10368 (8)	11619 (5)	5499 (4)
C8′	9145 (9)	11953 (6)	5433 (6)
C9′	11196 (10)	12309 (6)	5365 (5)
C10′	10591 (12)	11307 (6)	6214 (4)
C11′	12465 (7)	10345 (5)	3510 (4)
C12′	11959 (8)	10311 (6)	2799 (4)
C13′	13204 (8)	9601 (6)	3647 (6)
C14′	13220 (9)	11065 (6)	3588 (4)
CP1	8250 (6)	8608 (4)	3451 (3)
CP2	7452 (7)	9129 (5)	3714 (4)
CP3	6416 (7)	9254 (6)	3446 (4)
CP4	6083 (7)	8836 (6)	2875 (4)
CP5	6831 (7)	8302 (6)	2587 (4)
CP6	7869 (7)	8192 (5)	2862 (4)
CN1	4087 (7)	7488 (5)	4084 (4)
CN2	2858 (7)	7262 (7)	4218 (5)
CN3	6076 (7)	7108 (6)	4211 (4)
CN4	6948 (7)	6474 (7)	4347 (6)
CN5	4723 (8)	6158 (5)	3707 (5)
CN6	5033 (11)	6348 (7)	2976 (5)

[a] Numbers in parentheses are estimated standard deviations. [b] Atoms are labeled to agree with Figure 1.

some least-squares mean planes are provided as supplementary material.

Discussion

Synthesis. The anionic silicates **1** and **3** containing *tert*-butyl groups represent new substances. Silicate **1** was prepared analogously to that reported by Frye[20] for the preparation of the phenylsilicate **2** (eq 1). Silicate **3** was formed by first synthesizing

$$2(t\text{-Bu})_2C_6H_2(OH)_2 + PhSi(OMe)_3 + Et_3N \xrightarrow[CH_3CN]{CH_3OH} \underset{\mathbf{1}}{[((t\text{-Bu})_2C_6H_2O_2)_2SiPh][Et_3NH]} + 3MeOH \quad (1)$$

the triethylammonium salt that was then metathetically exchanged with tetraethylammonium chloride (eq 2).

$$2C_{10}H_6(OH)_2 + t\text{-BuSiCl}_3 + 4Et_3N \xrightarrow[\text{reflux}]{C_6H_6} [(C_{10}H_6O_2)_2Si\text{-}t\text{-Bu}][Et_3NH] + 3Et_3NH^+Cl^- \xrightarrow[Et_4N^+Cl^-]{\text{acetone}} \underset{\mathbf{3}}{[Et_4N][(C_{10}H_6O_2)_2Si\text{-}t\text{-Bu}]} + Et_3NH^+Cl^- \quad (2)$$

Carbon-13 NMR. There are very limited carbon-13 NMR studies on five-coordinated organosilicon compounds. The following are the results of the compounds studied in the present instance.

Table II. Selected Bond Lengths (Å) and Angles (deg) for Crystalline $[((t\text{-Bu})_2C_6H_2O_2)_2SiPh][Et_3NH]$ (**1**)[a,b]

	Lengths		
Si–O1	1.743 (5)	O1–C1	1.355 (8)
Si–O2	1.723 (5)	O2–C2	1.404 (8)
Si–O1′	1.821 (5)	O1′–C1′	1.375 (8)
Si–O2′	1.705 (5)	O2′–C2′	1.374 (8)
Si–CP1	1.868 (8)	N---O1′	2.803 (8)
	Angles		
O1–Si–O2	88.9 (2)	O1–C1–C2	112.2 (6)
O1–Si–O1′	167.9 (2)	O1–C1–C6	126.3 (6)
O1–Si–O2′	86.9 (2)	O2–C2–C1	112.0 (6)
O1–Si–CP1	97.2 (3)	O2–C2–C3	124.8 (6)
O2–Si–O1′	86.7 (2)	O1′–C1′–C2′	112.6 (6)
O2–Si–O2′	127.8 (3)	O1′–C1′–C6′	125.8 (6)
O2–Si–CP1	112.6 (3)	O2′–C2′–C1′	111.7 (6)
O1′–Si–O2′	86.9 (2)	O2′–C2′–C3′	122.4 (6)
O1′–Si–CP1	94.9 (3)	Si–CP1–CP2	124.4 (5)
O2′–Si–CP1	119.5 (3)	Si–CP1–CP6	121.8 (5)
Si–O1–C1	113.9 (4)	CN1–N---O1′	111.2 (6)
Si–O2–C2	112.7 (4)	CN3–N---O1′	109.9 (7)
Si–O1′–C1′	111.1 (4)	CN5–N---O1′	100.1 (6)
Si–O2′–C2′	116.0 (4)	Si–O1′---N	115.4 (4)

[a] Numbers in parentheses are estimated standard deviations. [b] Atoms are labeled to agree with Figure 1.

Table III. Atomic Coordinates in Crystalline $[(C_6H_4O_2)_2SiPh][Et_3NH]$ (**2**)[a]

atom type[b]	10^4x	10^4y	10^4z
Si	7244.6 (8)	8355.6 (4)	371.5 (7)
O1	6065 (2)	7897 (1)	−630 (1)
O2	8134 (2)	7673 (1)	681 (2)
O1′	8201 (2)	8659 (1)	1736 (2)
O2′	5927 (2)	8719 (1)	858 (2)
N	3569 (3)	7848 (1)	86 (2)
C1	6559 (3)	7327 (1)	−922 (3)
C2	7728 (3)	7197 (1)	−170 (3)
C3	8359 (3)	6633 (1)	−277 (3)
C4	7787 (4)	6197 (1)	−1191 (3)
C5	6628 (3)	6331 (2)	−1945 (3)
C6	5990 (3)	6902 (1)	−1830 (3)
C1′	7585 (3)	9118 (1)	2293 (3)
C2′	6285 (3)	9158 (1)	1798 (3)
C3′	5493 (3)	9593 (2)	2257 (3)
C4′	6054 (4)	9994 (2)	3250 (3)
C5′	7326 (4)	9956 (2)	3727 (3)
C6′	8131 (3)	9512 (2)	3274 (3)
C7	7839 (3)	8842 (1)	−894 (3)
C8	7098 (3)	8933 (2)	−2097 (3)
C9	7513 (4)	9304 (2)	−3026 (3)
C10	8698 (4)	9588 (2)	−2795 (3)
C11	9457 (3)	9512 (2)	−1622 (4)
C12	9033 (3)	9147 (1)	−687 (3)
CN1	3794 (3)	7641 (2)	1463 (3)
CN2	4650 (4)	7074 (2)	1692 (4)
CN3	2875 (3)	8468 (2)	−56 (4)
CN4	2977 (4)	8792 (2)	−1295 (5)
CN5	2958 (3)	7342 (2)	−810 (3)
CN6	1675 (4)	7123 (2)	−521 (4)
HN1	4358 (31)	7939 (14)	−136 (26)

[a] Numbers in parentheses are estimated standard deviations. [b] Atoms are labeled to agree with Figure 2.

The carbons attached to the oxygen atoms of the aromatic diols appear most downfield and lie in a narrow range. This is most certainly because of the greater electronegativity of the oxygen atoms to which they are attached. In the case of compound **1**, because of the unsymmetrical nature of the aromatic diol, two signals are observed.

The chemical shifts of the phenyl ring in compounds **1** and **2** are in the order ipso > ortho > para ~ meta. Harris[18a] et al. have studied the ^{13}C NMR of 1-phenylsilatrane and observed a similar trend. Rakita[18b–d] and co-workers have studied the ^{13}C

Table IV. Selected Bond Lengths (Å) and Angles (deg) for $[(C_6H_4O_2)_2SiPh][Et_3NH]$ (**2**)[a,b]

Lengths

Si–O1	1.785 (2)	O1′–C1′	1.351 (3)
Si–O2	1.720 (2)	O2′–C2′	1.370 (3)
Si–O1′	1.748 (2)	N–HN1	0.92 (3)
Si–O2′	1.727 (2)	HN1- - -O1	1.94 (3)
Si–C7	1.871 (3)	N- - -O1	2.840 (3)
O1–C1	1.364 (3)	HN1- - -O2′	2.45 (3)
O2–C2	1.372 (3)	N- - -O2′	3.089 (3)

Angles

O1–Si–O2	87.95 (9)	O1–C1–C2	112.2 (2)
O1–Si–O1′	161.1 (1)	O2–C2–C1	113.0 (3)
O1–Si–O2′	84.56 (9)	O2–C2–C3	125.7 (3)
O1–Si–C7	98.5 (1)	O1′–C1′–C6′	126.1 (3)
O2–Si–O1′	85.7 (1)	O1′–C1′–C2′	112.8 (2)
O2–Si–O2′	138.6 (1)	O2′–C2′–C3′	126.6 (3)
O2–Si–C7	111.4 (1)	O2′–C2′–C1′	112.2 (3)
O1′–Si–O2′	89.5 (1)	Si–C7–C8	121.9 (2)
O1′–Si–C7	100.3 (1)	Si–C7–C12	122.0 (2)
O2′–Si–C7	109.9 (1)	N–HN1- - -O1	165 (3)
Si–O1–C1	111.1 (2)	N–HN1- - -O2	127 (2)
Si–O2–C2	112.6 (2)	CN1–N–HN1	107 (2)
Si–O1′–C1′	111.9 (2)	CN3–N–HN1	104 (2)
Si–O2′–C2′	112.0 (2)	CN5–N–HN1	107 (2)
O1–C1–C6	126.3 (3)		

[a] Numbers in parentheses are estimated standard deviations. [b] Atoms are labeled to agree with Figure 2.

Table V. Atomic Coordinates in Crystalline $[(C_{10}H_6O_2)_2Si\text{-}t\text{-}Bu][Et_4N]$ (**3**)[a]

atom type[b]	10^4x	10^4y	10^4z
Si	9016 (2)	1795.6 (9)	6979 (1)
O1	8205 (4)	2257 (2)	5938 (3)
O2	9181 (5)	2304 (2)	7915 (3)
O1′	10506 (5)	1522 (2)	8007 (3)
O2′	9780 (5)	1537 (2)	6032 (3)
N	7303 (5)	6897 (2)	2906 (4)
C1	7846 (7)	2706 (3)	6328 (5)
C2	8423 (7)	2741 (3)	7489 (5)
C3	8197 (7)	3185 (3)	8022 (5)
C4	7378 (8)	3605 (3)	7440 (6)
C5	7104 (9)	4063 (3)	7980 (6)
C6	6275 (11)	4447 (4)	7425 (8)
C7	5693 (10)	4428 (3)	6288 (8)
C8	5955 (9)	4002 (3)	5722 (6)
C9	6788 (8)	3576 (3)	6276 (5)
C10	7043 (8)	3121 (3)	5743 (5)
C1′	11277 (8)	1181 (3)	7616 (6)
C2′	10859 (8)	1185 (3)	6461 (5)
C3′	11527 (8)	860 (3)	5908 (6)
C4′	12667 (8)	529 (3)	6492 (6)
C5′	13391 (9)	192 (3)	5975 (7)
C6′	14480 (9)	−128 (3)	6527 (7)
C7′	14932 (8)	−129 (3)	7649 (8)
C8′	14262 (9)	193 (3)	8205 (7)
C9′	13101 (8)	532 (3)	7655 (6)
C10′	12383 (8)	855 (3)	8197 (6)
C11	7473 (8)	1362 (3)	7023 (6)
C12	6080 (12)	1514 (6)	6202 (16)
C13	7698 (16)	820 (5)	6812 (17)
C14	7187 (20)	1390 (5)	8046 (13)
CN1	6476 (10)	7063 (5)	3640 (8)
CN2	7170 (16)	7545 (6)	4390 (10)
CN3	8839 (9)	6732 (5)	3571 (8)
CN4	8960 (13)	6267 (4)	4382 (7)
CN5	6546 (13)	6442 (4)	2226 (10)
CN6	7284 (17)	6218 (6)	1430 (9)
CN7	7420 (14)	7359 (5)	2156 (11)
CN8	5946 (12)	7559 (5)	1361 (8)

[a] Numbers in parentheses are estimated standard deviations. [b] Atoms are labeled to agree with Figure 3.

Table VI. Selected Bond Lengths (Å) and Bond Angles (deg) in Crystalline $[(C_{10}H_6O_2)_2Si\text{-}t\text{-}Bu][Et_4N]$ (**3**)[a,b]

Lengths

Si–O1	1.769 (5)	O1–C1	1.335 (8)
Si–O2	1.739 (5)	O2–C2	1.349 (8)
Si–O1′	1.769 (5)	O1′–C1	1.341 (8)
Si–O2′	1.742 (5)	O2′–C2′	1.354 (8)
Si–C11	1.871 (7)		

Angles

O1–Si–O2	87.2 (2)	Si–O2–C2	114.0 (4)
O1–Si–O1′	153.3 (2)	Si–O1′–C1′	113.0 (4)
O1–Si–O2′	84.3 (2)	Si–O2′–C2′	113.8 (4)
O1–Si–C11	108.4 (3)	O1–C1–C2	112.7 (6)
O2–Si–O1′	83.8 (2)	O1–C1–C10	127.7 (6)
O2–Si–O2′	143.0 (3)	O2–C2–C3	128.5 (6)
O2–Si–C11	108.4 (3)	O2–C2–C1	111.1 (7)
O1′–Si–O2′	87.3 (2)	O1′–C1′–C2′	112.4 (6)
O1′–Si–C11	102.6 (3)	O1′–C1′–C10′	127.8 (8)
O2′–Si–C11	108.5 (3)	O2′–C2′–C3′	127.6 (6)
Si–O1–C1	112.6 (4)	O2′–C2′–C1′	111.5 (7)

[a] Numbers in parentheses are estimated standard deviations. [b] Atoms are labeled to agree with Figure 3.

NMR of phenylsilanes in some detail. Their studies suggest that if resonance effects dominate, the most affected carbons of the phenyl ring are ortho and para. In the present study, it is observed that meta and para carbons are almost unaffected, indicating that the dominant effects may be inductive. However, it is to be noted that the chemical shifts of C_{ipso} and C_o are affected by other factors as well, e.g., steric and magnetic anisotropy of the neighboring groups.[19]

Another feature worth mentioning is that the chemical shifts of the various groups seem to be largely unaffected by the geometry at silicon, although the ipso carbons of the diol and the phenyl ring of compounds **2** and **3**, which have solid-state structures more displaced toward the rectangular pyramid, appear slightly more downfield than those of compound **1**. This may be because of a rapid interconversion in solution between the RP and TBP structures or because the chemical shifts may be largely affected by the general arrangement of substituents around silicon, which, in all the compounds in the present study, are the same, viz., four oxygens and one carbon.

Basic Structures. Except for the *t*-Bu groups, the three anions have a pseudo-2-fold axis coincident with the Si–C bond. To facilitate examination of this pseudosymmetry, the atom-labeling schemes are such that primed atoms go into the unprimed ones by this pseudo-2-fold axis.

For all three compounds, the geometry about the Si atom lies on the coordinate connecting a trigonal bipyramid (TBP) having O1 and O1′ in axial positions and a rectangular pyramid (RP) having four basal oxygen atoms and an apical carbon atom, where the carbon atom is pivotal in the Berry pseudorotation process.[27] Using the dihedral angle method[7] to assess displacement, **1** is displaced 26.8% (29.0% using unit vectors) from the TBP toward the RP. For **2** and **3** these values are 56.8% (59.4% using unit vectors) and 77.9% (80.3% using unit vectors), respectively.

In **1** and **2** there is a hydrogen bond between the amino hydrogen atom of the cation and an axial oxygen atom of the anion. In **1**, where hydrogen atoms could not be located, the hydrogen bond is inferred from the non-hydrogen atom geometry. Evidence for this hydrogen bond is seen both in the Si–O bond lengths and in the cation–oxygen geometry. The distance between N and O1′ is 2.803 (8) Å, which is less than the van der Waals sum of 3.0 Å.[28] The angles CN1–N- - -O1′, CN3–N- - -O1′, and CN5–N- - -O1′ have nearly tetrahedral values of 111.2 (6), 109.9 (7), and 100.1 (6)°, respectively, which indicates that the amino hydrogen atom is directed toward O1′. The angle Si–O1′- - -N is 115.4 (4)°, which suggests that a lone pair on O1′ could be directed toward the N atom.

We have observed[3,4] that a hydrogen bond to a ligand oxygen atom increases the central atom to ligand bond distance. In this case, the Si–O1′ bond length of 1.821 (5) Å, which is considerably longer than the other axial bond Si–O1, having a value of 1.743

---

(27) Berry, R. S. *J. Chem. Phys.* **1960**, *32*, 933.

Table VII. Axial and Equatorial Angles (θ) and Dihedral Angle (δ) Sums for Pentacoordinated Anionic Silicates (deg)

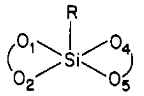

no.	δ_{24}[a]	θ_{15}	θ_{24}	Si–O$_{ax}$,[b] Å	Si–O$_{eq}$,[b] Å	Δ(ax − eq), Å	%(TBP → RP)[c]	ref[d]
1	37.3	167.9	127.8	(1) 1.734	(2) 1.723	0.011	29.0	this work
				(5) 1.821[f]	(4) 1.705			
7	36.5	168.3	129.1	(1) 1.763	(2) 1.700	0.063	30.8	29
				(5) 1.789	(4) 1.708	0.081		
10A[e]	26.2	168.4	141.2	(1) 1.734	(2) 1.684	0.050	53.6	31
				(5) 1.689	(4) 1.683	0.006		
10B[e]	17.0	163.7	146.4	(1) 1.732	(2) 1.688	0.044	70.8	31
				(5) 1.707	(4) 1.692	0.015		
2	21.7	161.1	138.6	(1) 1.785[f]	(2) 1.720		59.4	this work
				(5) 1.748	(4) 1.727	0.021		
8[g]	19.8	159.4	139.0	(1) (5) 1.78	(2) (4) 1.729	0.05	63.8	29
3	10.1	153.3	143.0	(1) 1.769	(2) 1.739	0.030	80.3	this work
				(5) 1.769	(4) 1.742	0.027		
9	4.4	151.0	146.7	(1) 1.772	(2) 1.736	0.036	91.4	29
				(5) 1.759	(4) 1.752	0.007		

[a] The dihedral angle δ_{24} is the one between triangular faces 124 and 245 containing the common equatorial edge 24. [b] The numbers in parentheses are atom identification relative to the structure given below the table heading. [c] Based on unit bond distances.[7] [d] These are references to the X-ray studies. [e] There are two independent molecules per unit cell for **10**. [f] The oxygen atom of these Si–O ring bonds is also hydrogen bonded to the Et_3NH^+ cation. [g] Compound **8** contains a crystallographic 2-fold axis coincident with the silicon atom.

(5) Å, is further evidence of a hydrogen bond to O1′.

The hydrogen-bonding geometry in **2** is very similar to that found in **1**. In this case the amino hydrogen atom was included in the refinement. The distance HN- - -O1 is 1.94 (3) Å, which is considerably less than the van der Waals sum of 2.7 Å.[28] Once again, comparison of the axial Si–O bond lengths shows a longer bond to the oxygen atom that is involved in hydrogen bonding. The distance Si–O1 is 1.785 (2) Å while the distance Si–O1′ is 1.748 (2) Å.

Structural Comparisons. The composition of the anionic phenylsilicates **2** and **4** differs only in the type of cation present, yet their structures are displaced considerably from each other. The presence of hydrogen bonding between the Et_3NH^+ ion and one of the silicate oxygen atoms (O1) apparently is responsible for the greater rectangular-pyramidal character of **2** (59.4%) compared to the 29.5% displacement from the TBP toward the RP found for **4**[16] which lacks hydrogen bonding. Since hydrogen bonding always causes an increase in the length of the Si–O bond of the affected oxygen atom,[4] a likely explanation for the structural shift toward the RP resides with the change in electron density expected in the framework bonds. As a result of the partial removal of electron density from the oxygen atom participating in hydrogen-bond formation, lessened Si–O bond pair repulsions may occur. The reduction in bond pair repulsions would tend to stabilize the normally higher energy RP form.

In any event, other examples of this hydrogen-bonding influence for five-coordinated silicon compounds show a similar structural displacement toward the rectangular pyramid.[3,4,29,30] Comparison of the structures of **3**, studied here, and **5**,[4] having naphthalene units that comprise the spirocyclic system, shows that **5** assumes a nearly ideal RP structure (97.6%). The structural distortion for **3** is 80.3% toward the RP. One would expect that the presence of the acyclic *tert*-butyl group in **3**, due to its large steric size and low electronegativity,[6,14,15] would allow a greater preference toward the RP compared to the influence of the phenyl group in **5**. Thus, the hydrogen-bonding influence appears to overbalance the structural effects typically associated with the acyclic ligand in favoring the formation of the rectangular pyramid. Although the latter "rule" concerning the size and electronegativity of the acyclic ligand in stabilizing a RP was formulated for phosphoranes,[6,14,15] as the accompanying paper shows,[29] it applies to five-coordinated anionic silicon compounds as well. A direct comparison of the hydrogen-bond effect is found between the structures of the anionic silicate derivatives, **6**[4] and **7**,[29] both of which have the 1-naphthyl group in the fifth position. The derivative containing the hydrogen-bonding pyridinium cation, **6**, again has its geometry[4] shifted toward the rectangular pyramid.

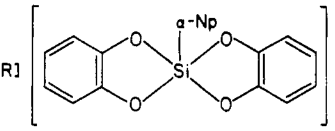

6, $R = C_5H_5NH$ (58.7)
7, $R = Et_4N$ (30.8)

The tetra *tert*-butyl phenylsilicate, **1**, possessing an Et_3NH^+ cation, has a structure displaced 29.0% toward the rectangular pyramid compared to the 59.4% displacement found for the related unsubstituted catecholate, $[(C_6H_4O_2)_2SiPh][Et_3NH]$ (**2**). The *tert*-butyl ring substituents in **1** provide two effects, both favoring the trigonal bipyramid. The inductive effect is expected to enhance Si–O bond pair repulsions and increase the energy difference between the trigonal bipyramid and the less stable rectangular pyramid.[3,14] The large size of the *tert*-butyl groups acts to shield the anionic silicate portion from the geometrical consequences of the anion–cation charge interaction as well as those resulting from the presence of the hydrogen bond.

Distortion Coordinate. With the availability of the structures of the newly formed five-coordinated anionic silicates, **1**–**3**, and those in the accompanying paper,[29] **7**–**9**, as well as that reported by Schomburg,[31] **10**, it is of interest to more firmly establish the form of the distortion coordinate followed by these derivatives.

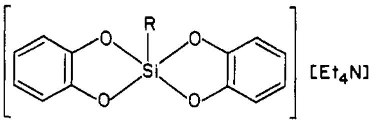

8, R = *n*-Bu (63.8%)
9, R = *t*-Bu (91.4%)

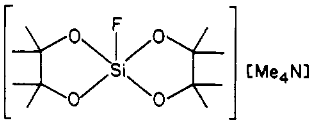

10 (53.6%, 70.8%)

---

(28) Bondi, A. *J. Phys. Chem.* **1964**, *68*, 441.

(29) Holmes, R. R.; Day, R. O.; Chandrasekhar, V.; Harland, J. J.; Holmes, J. M. *Inorg. Chem.*, following paper in this issue.

(30) Schomburg, D. *Z. Naturforsch., B: Anorg. Chem., Org. Chem.* **1982**, *37B*, 195.

(31) Schomburg, D. *Z. Naturforsch.*, **1983**, *B: Anorg. Chem., Org. Chem.* *38B*, 938.

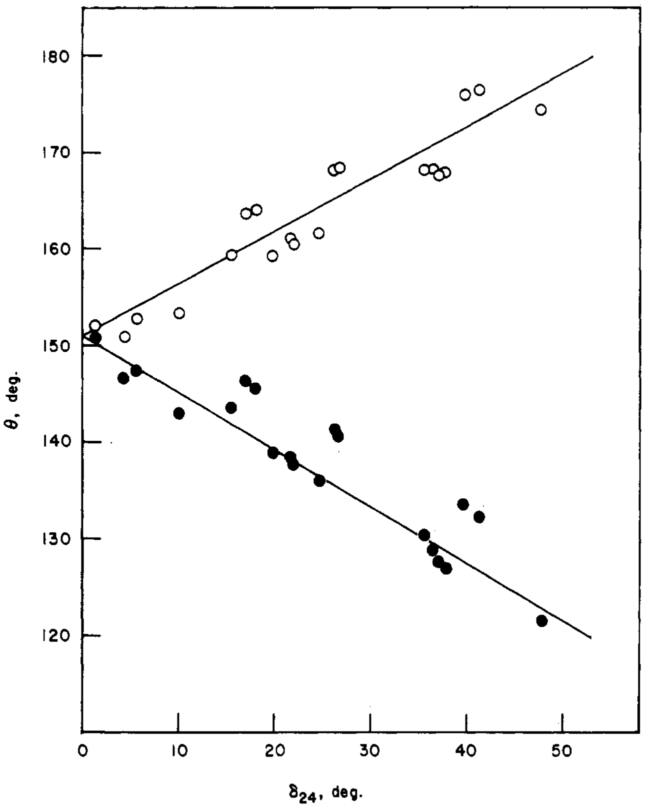

Figure 4. Variations of the axial angle, θ_{15} (open circles), and equatorial angle, θ_{24} (filled circles), vs. the dihedral angle δ_{24} as structural distortion for pentacoordinated silicon(IV) compounds listed in Table VII and in Table IV of ref 3 proceeds along the Berry coordinate from a rectangular pyramid toward a trigonal bipyramid. The least-squares lines $\theta_{15} = 0.5697\delta_{24} + 150.0$ and $\theta_{24} = -0.5778\delta_{24} + 151.9$ give an average value of 151.0° for the trans basal angle of the "limiting" rectangular pyramid. The solid lines were determined by the values of 180 and 120° for the ideal trigonal bipyramid, $\delta_{24} = 53.1°$, and 151.0° at $\delta_{24} = 0$.

By the dihedral angle method,[32] the data summarized in Table VII are plotted in Figure 4. As with similar data previously available for anionic silicates,[3,4] the structures span the range between the ideal trigonal bipyramid ($\delta_{24} = 53.1°$) and the rectangular pyramid ($\delta_{24} = 0°$). The solid lines are determined by the θ values for the ideal trigonal bipyramid at $\delta_{24} = 53.1°$ and the θ value of 151° for the "limiting" rectangular pyramid. The latter value is obtained from a least-squares fit of the axial and equatorial θ angles. These equations are given in the caption for Figure 4. It is seen that the distortion coordinate closely follows that expected from the Berry pseudorotational process,[27] which leads to a square-pyramidal barrier structure having a trans basal angle of 150°.

This structural correlation for five-coordinated silicon compounds parallels that of phosphoranes[6,7,17] and also the structural distortions observed more recently in a series of cyclic arsoranes.[1,10] The ease of structural distortion of anionic silicates related to substituent and lattice effects implies a high degree of molecular nonrigidity for these pentacoordinated derivatives.

In the ideal trigonal bipyramid, we estimated[4] a 1.78-Å distance for the axial Si–O bond length and 1.68 Å for the equatorial Si–O length. As apparent in Table VII, there is a general convergence in these lengths in terms of the difference between axial and equatorial Si–O bond distances, Δ, as δ_{24} goes from 53.1° (for the TBP) to 0° (for the RP). Additional data on this point is found for compounds **6**, **8**, **10**, **12**, and **13** listed in Table V of ref 4, which follows the same trend showing Δ approaching near zero as the RP is reached. Since hydrogen bonding causes a lengthening of the affected Si–O bonds, these bonds should not be included in a consideration of this trend.

Acknowledgment. The support of this research by the National Science Foundation (Grant CHE8205411) is gratefully acknowledged, as is an NSF grant for the purchase of the Varian XL-300 NMR spectrometer. We also thank the University of Massachusetts Computing Center for generous allocation of computer time.

Registry No. **1**, 96292-62-5; **2**, 96306-47-7; **3**, 96292-64-7; 3,5-di-*tert*-butylcatechol, 1020-31-1; phenyltrimethoxysilane, 2996-92-1; catechol, 120-80-9; *tert*-butyltrichlorosilane, 18171-74-9; 2,3-naphthalenediol, 92-44-4; tetraethylammonium chloride, 56-34-8.

Supplementary Material Available: Table A, anisotropic thermal parameters for **1**; Table B, fixed hydrogen atom parameters for **1**; Table C, anisotropic thermal parameters for **2**; Table D, fixed hydrogen atom parameters for **2**; Table E, anisotropic thermal parameters for **3**; Table F, fixed hydrogen atom parameters for **3**; Table G, additional bond lengths and angles for **1**; Table H, additional bond lengths and angles for **2**; Table I, additional bond lengths and angles for **3**; Table J, deviations from least-squares mean planes for **1**; Table K, deviations from least-squares mean planes for **2**; Table L, deviations from least-squares mean planes for **3**; and a listing of observed and calculated structure factor amplitudes for **1**–**3** (41 pages). Ordering information is given on any current masthead page.

---

(32) Muetterties, E. L.; Guggenberger, L. J. *J. Am. Chem. Soc.* **1974**, *96*, 1748.